11

Armless Climbing and Walking in Robotics

Maki K. Rashid
Mechanical and Industrial Engineering, Sultan Qaboos University, Muscat
Sultanate of Oman

1. Introduction

Climbing and walking robots perform tasks that are too difficult, dangerous or time consuming for the human worker. These tasks can be inspection work in hazardous or unpleasant environments (Briones et al., 1994) and, (Xu & Ma, 2002), military, maintenance (Tokioka & Sakai, 1988), overhauling (Yanzeng et al., 1999), manufacturing (Shuliang et al., 2000), and search and rescue works. With all progress in the development of climbing and walking techniques such robots still haven't been able to penetrate the service market. There are two reasons for this slow down: First, most of today's commercially available climbing and walking robots have insufficient payload-to weight ratio. Second, all of the most recent developments have been engineered for one very specific task. But the customer demand new approach in robot development. Mainly such robots must be competitive with other solutions by conducting the task economically. Moreover the climbing and walking robots should also be able to perform a variety of tasks so that the return of investment for the customer is improved.

Armless robot without articulated hand or legs requires holding technique to working surfaces. Several types of attachment mechanisms have been studied and developed for climbing and walking robots. In the case of workspace that contains structural elements that support the use of mechanical fasteners or grippers then the contact to the surface can be established through a positive connection. This type of adhesion mechanism is the grasping technique, which requires holds, spines or grooves to grasp and pull the whole body upwards, however the climbing down process is challenging for this method (Bretl et al., 2003) and, (Autumn et al., 2000). For rough surfaces, this is a quite powerful technique but it is not suitable for armless robot. In addition if the surface is flat and smooth, this method cannot be applied. Most of today's robotic applications demand highly flexible solutions able to move the robot autonomously without the need of grasping a predefined elements. Therefore, the states of the art of armless robots developed an adhesive force method for climbing surfaces. Such force can be generated using different tactics. The most common type is the suction adhesion, where the robot carries an on-board pump to create vacuum inside cups which are pressed against the wall or ceiling (Pack et al., 1997) and, (Nagakubo et al., 1994). Such attachment suffers from the time delay in developing the vacuum and the special requirements for smooth surfaces and sealing design. In addition, power consumption is too high during attachment. Finally, the suction adhesion mechanism relies on ambient pressure to stick on wall, and therefore it is not useful in applications that require near zero surrounding pressure as in the case of space application.

Source: Bioinspiration and Robotics: Walking and Climbing Robots, Book edited by: Maki K. Habib
ISBN 978-3-902613-15-8, pp. 544, I-Tech, Vienna, Austria, EU, September 2007

Another common type of adhesion mechanism is the magnetic adhesion (Rashid & Khalil, 2004) and, (Shuliang et al., 2000). Magnetic adhesion has been implemented in wall climbing robots for specific applications such as petrochemical and nuclear facility inspection. This is reliable in specific cases where surfaces allow magnetic attachment. Magnetic wheels usually used for inspecting curved surfaces despite that, magnetic attachment is useful only in specific environments where the surface is ferromagnetic. In addition, the power consumption of magnetic adhesion could be extremely high.
A recent technique of adhesion is inspired by Geckos' ability to climb surfaces under wet or dry and smooth or rough conditions. This type of attachment has been attracted scientist's attention for decades. The mechanism of this adhesion is generated by the compliant micro/nano-scale high aspect ratio beta-keratin structures at Gecko feet. They can manage to adhere to almost any surface with a controlled contact area (Autumn et al., 2000). It has been shown that adhesion is mainly due to molecular forces such as van der-Waals forces (Autumn et al., 2002). Researchers have created a robot that can run up a wall as smooth as glass and onto the ceiling by using a new gecko like, ultra sticky fiber adhesive attached to its feet or wheels (Shah & Sitti, 2004).
Finally the most common adhesion mechanism in robotic is the frictional forces due to the contact surface loads. Such mechanism appears in both wheeled (Iagnemma & Dubowsky, 2004) and legged robots. Although wheeled mechanisms are relatively efficient, easy to steer, and suited for high-speed driving in many applications. They are, however, not effective in rugged environments such as rough and/or muddy terrains. In some cases legs can provide higher terrain adaptability than wheels but some researchers are targeting higher terrain adaptability by using multilink articulated robots that "crawl" like snakes (Hirose, 1993).
This chapter emphasises the development of an intelligent controller to stabilize an armless single wheel walking/climbing robot by using the computer simulation. The stabilization mechanism for a single wheel mobile robot attracted researcher attentions in robotic area (Rashid, 2007). A simulation platform is developed in this work for testing different control tactics for achieving the required stabilization for single wheel mobile robot as a cost effective procedure. The graphic representation of the robot, the dynamic solution, and, the control scheme are all integrated on a common computer platform using Visual Basic. Simulation indicates the possibility of substantial control of such robot without knowing prior details about the internal structure or resulted dynamic behaviour. It is done just by looking at the dynamic manners and using manual operation tactics. Then, twenty five rules are extracted and implemented using Takagi-Sugeno's fuzzy controller with significant achievement in controlling robot motion during simulation. The resulted data from the successful implementation of this fuzzy model subsequently used to train a neurofuzzy controller using ANFIS scheme to provide further improvement in robot performance.

2. Armless Intelligent Single Wheel Mobile Robot

Self-stabilization of a single rolling wheel using a gyroscopic actuation was under several explorations for its importance in robotic applications (Nandy & Xu, 1998) and (Xu et al., 1999). The mechanical design consists basically of a gyro disk attached to internally suspended pendulum. Such arrangement provides a forward and reverse movement in which the reaction of the applied motor torque is counteracted by the moment of the hanging mass of the gyroscope and gimbals system as shown in Figures 1 and 2. The

spinning gyro of the pendulum mechanism provides the turning, as well as the static and dynamic balance using the effect of gyroscopic precession induced by the applied torque.

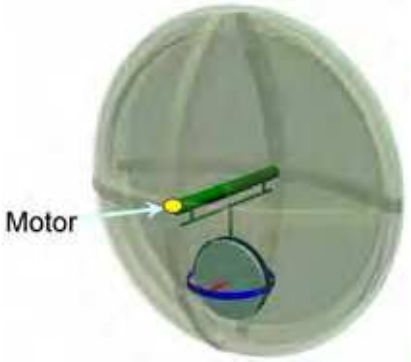

Figure 1. The Basic Design for the Gyroscopic Wheel

Recent studies (Martynenko & Formal'skii, 2005) developed methodolgy to control the longitudinal motion of a single wheel robot on an uneven surface. Yangsheng & Samuel, (2004) developed a linear state feedback approach to stabilize a robot at any desired lean angle. A prototype is developed by Ferreira et al., (2000) and Cavin, (2001) for a single-wheeled autonomous vehicle capable of righting itself from any position, spinning about its own axis, moving forward and backward, and avoiding obstacles in its path. The platform gained feedback from the environment using a tilt sensor and electronic compass for both balancing and heading. It also included speed detection and object avoidance by using sonar sensor and shaft encoder on the main drive motor. It is demonstrated experimentally that the wheel can automatically be controlled by using the learned human control input (Samuel et al., 2001). Cost of such experimental setups might represent a burden for the investigators in this area. The present work is targeting simulation tools and techniques that might result in lowering such price tag by using virtual prototyping and real time simulation in controlling such system under different manoeuvring tasks using intelligent control scheme. Visual Basic is utilized as a medium for integrating all of these components. A neural network can approximate the response, but is not capable of interpreting the results in terms of natural language. Therefore, using the neural networks and fuzzy logic in the controller design via neurofuzzy would provide both learning and response readability.

3. Computer Simulation and Governing Equations

Virtual prototyping and real time simulation are carried out by integrating different computer programs under Windows environment using Visual Basic.

3.1 Robot graphical modelling

The graphical representation of the outside shells and the gyro-pendulum are shown in Figure 2. All generated parts for the single wheel robot are drafted in separate part files. The outside shells are considered as the basic parts in the generated assembly file. All other parts are externally referenced to this assembly file and appropriate constraints between parts and sub-assemblies are added to control the motion as required.

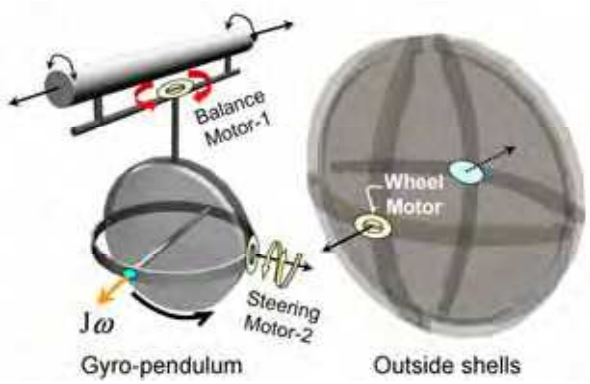

Figure 2. The Graphical Model for the Robot

3.2 Real time motion simulation

After the check for possible interference in graphical modelling from previous step, the graphical assembly file is exported to the motion simulation software. However, the motion simulator may mistakenly recognise some constraints. Such constraints are then corrected, and the system motion is appropriately verified. All motion coordinates for the moving wheel and the gyro-pendulum suspension system in the simulation file are assigned in a way similar to that of the derived equations in this work to simplify the extraction of results. The dynamic equations are programmed by using the visual basic to investigate the robot motion as a result of specific external effects (as clarified in Figure 3).

3.3 The governing equations

The motion and the stabilizing actions of the wheel are based on the gyroscopic precession principle. Due to its angular momentums the wheel tends to precess at right angles with the externally applied torque. The fundamental equation of the gyroscopic precession is:

$$T = I \; x \; \omega \; x \; \Omega \tag{1}$$

where T is the torque acting on the gyroscope, $I\omega$ is its angular momentum and Ω is the precession rate.

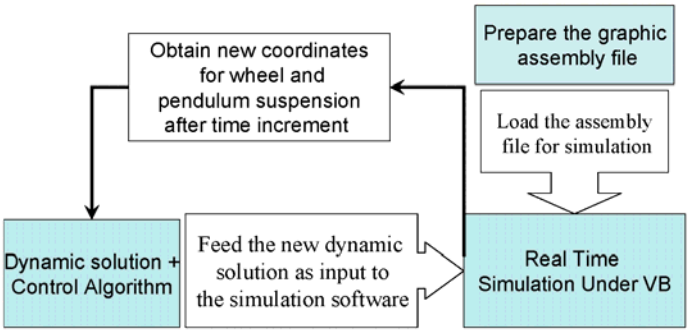

Figure 3. Solution and simulation steps for the Gyro-stabilizing Wheel

When the robot wheel forward velocity is zero, the gyroscopic effect of the flywheel can stop the robot from falling over by using the balance motor-1 in figure 2 and simultaneously induces a positive rotation around the robot vertical axis. The tilt motor-2 can be used to steer the robot to the required direction, which cause the wheel to lean to one side. The formulations of the fundamental dynamic equations are based on Lagrangian constrained generalized principle (Xu et al., 1999). Other methods can be applied without using Lagrange multipliers to reduce computation complexity (Nukulwuthiopas et al., 2002). More details are available for modelling a dynamic system subjected to nonholonomic constraints (Bloch, 2003)

It is more convenient to formulate this problem by assigning four coordinate frames as shown in Figure 4. These frames are used to relate the values of the dynamic variables from all other coordinates to the absolute coordinates *XYZ*.

α , α_G	Precession angles of the wheel and gyro-flywheel respectively measured about the vertical axis
β	Definition Lean angle of the wheel measured between the rotation axis and the vertical
β_G	Angle between the pendulum link l and Z_G-axis of the gyro-flywheel
γ, γ_G	Spin angles of the wheel and gyro-flywheel respectively
m_w, m_P, m_G	Effective masses of the wheel, pendulum mechanism, and gyro-flywheel
m_T	Total effective mass of the robot
g	Gravitational acceleration

Table 1. Variable definitions

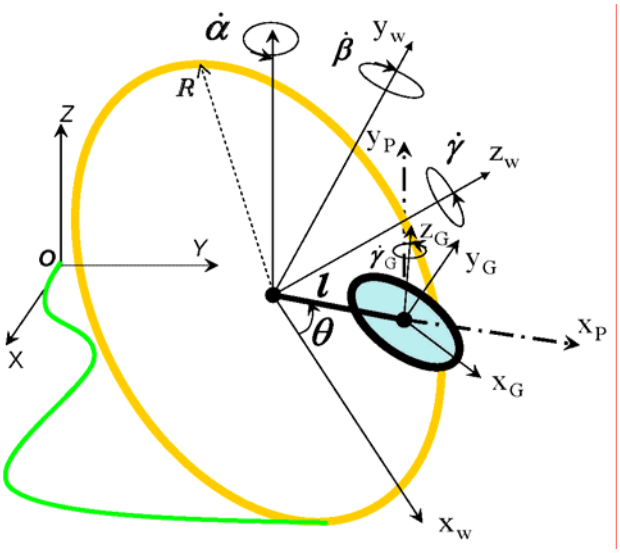

Figure 4. Reference frames and system variables

Table 1 describes the notation for the parameters that used in formulating the dynamic equations. The assigned four coordinates are the following: i) the absolute coordinates *XYZ* whose x-y plane is attached to the wheel surface; ii) the wheel centre body coordinate frame $\{x_w, y_w, z_w\}$ where the z_w represents the wheel rotation axis; iii) the coordinate frame of the suspended pendulum mechanism is $\{x_p, y_p, z_p\}$ centred at the gyro-flywheel attachment; iv) the gyro-flywheel coordinate frame $\{x_G, y_G, z_G\}$ centred at the gyro-flywheel attachment and z_G represents the gyro axis of rotation. The dynamic modelling of the robot is based on the assumptions that all of the components are rigid. Roll/slip condition for the wheel is checked continuously using a reasonable coefficient of friction between the wheel and the floor. Angular velocity of the gyro is kept constant and, both robot wheel and gyro-flywheel are modelled assuming axial symmetry. Interaction between surface irregularities and wheel surface is not incorporated in the modelling.
Assuming that the vectors in the absolute and wheel body coordinates are having scalar components (X, Y, Z) and (x_w, y_w, z_w) respectively then,

$$\begin{bmatrix} X \\ Y \\ Z \end{bmatrix} = R_0^w \begin{bmatrix} x_w \\ y_w \\ z_w \end{bmatrix} \tag{2}$$

where R_0^w is a (3x3) real matrix of directional cosines that transforms the coordinate of the vectors from the frame $x_w y_w z_w$ Cartesian system to the absolute frames *XYZ* systems. Because of space limitation, the detailed derivation of such matrix transformation can be found in Xu et al., (1999). In the problem formulation the assumed constrains of rolling without slipping has produced a non-holonomic system with some non-integrable equations. Applying the constrained kinematics equations and incorporating equation (2) for coordinate transformation attains the non-integrable Equations (3) and (4), and the integrable equation (5):

$$\dot{X} = R(\dot{\gamma}\cos\alpha + \dot{\alpha}\cos\alpha\cos\beta - \dot{\beta}\sin\alpha\sin\beta) \tag{3}$$

$$\dot{Y} = R(\dot{\gamma}\sin\alpha + \dot{\alpha}\sin\alpha\cos\beta + \dot{\beta}\cos\alpha\sin\beta) \tag{4}$$

$$\dot{Z} = R\dot{\beta}\cos\beta \tag{5}$$

If υ_w and ω_w are respectively set to represent the linear and the angular velocity of the robot wheel centre of mass with respect to the absolute coordinates, then through the coordinate transformation matrices we can obtain a vector equation for ω_w and from the no slip kinematics and equation (6) we can attain the set of Equations (3-5):

$$\upsilon_w = \dot{X}i + \dot{Y}j + \dot{Z}k \tag{6}$$

By integrating equation (5) we get,

$$Z = R\sin\beta \tag{7}$$

The Lagrangian constrained generalized principle is one of the techniques used for analyzing the non-holonomic systems as in this work to derive the dynamic model for the

gyroscopic wheel. Let us consider a non-holonomic system with n degrees of freedom, whose Lagrangian coordinates and velocities are q_j, and, $\dot{q}_j$, (j = 1, 2,..., m). If the system is subjected to a set of generalized forces, given by Q_j, (j = 1, 2, ..., m), then there will be (m-n) constrained conditions that must be explicitly satisfied by the system. The constrained equations can be written as,

$$f_s = f_s(\mathbf{q},t) = f_s(q_1,q_2,...,q_m,t) = 0 \tag{8}$$

For nonholonomic system, the set of Lagrangian equations are then given by,

$$\frac{d}{dt}\left(\frac{\partial L}{\partial \dot{q}_j}\right) - \frac{\partial L}{\partial q_j} = \sum_{s=1}^{m-n} \lambda_s . \frac{\partial}{\partial q_j} f_s(\mathbf{q},t), \quad j = (1,2,....,m) \tag{9}$$

where, $L = T - P$ is the Lagrangian function, T is the total kinetic energy of the system, P is the total potential energy of the system, and λ_s is a Lagrangian multiplier that accounts for the system constraints.

The system can be divided into three parts namely robot wheel, pendulum mechanism, and, gyro-flywheel. The kinetic energy of the robot wheel is,

$$\begin{aligned} T_w = {} & \frac{1}{2} m_w [\dot{X}^2 + \dot{Y}^2 + (R\dot{\beta}\cos\beta)^2] \\ & + \frac{1}{2}[I_{xxw}(\dot{\alpha}\sin\beta)^2 + I_{yyw}\dot{\beta}^2 + I_{zzw}(\dot{\alpha}\cos\beta + \dot{\gamma})^2 \end{aligned} \tag{10}$$

The potential energy of the robot wheel is

$$P_{\mathrm{w}} = m_{\mathrm{w}} g R \sin\beta \tag{11}$$

The translational and the rotational kinetic energy of the internal mechanism and the flywheel are derived by applying the transformation relation between the centre of robot wheel absolute coordinates to the gyro-flywheel centre (x_G, y_G, z_G) described as,

$$\begin{bmatrix} \mathrm{x_G} \\ \mathrm{y_G} \\ \mathrm{z_G} \end{bmatrix} = \begin{bmatrix} \mathrm{X} \\ \mathrm{Y} \\ \mathrm{Z} \end{bmatrix} + \mathrm{R}_{\mathrm{w}}^{\mathrm{O}} \begin{bmatrix} \iota\cos\theta \\ \iota\sin\theta \\ 0 \end{bmatrix} \tag{12}$$

The translational kinetic energy of the flywheel and the pendulum mechanism T_G^t can be expressed as:

$$T_{\mathrm{G}}^{\mathrm{t}} = \frac{1}{2}(m_{\mathrm{P}} + m_{\mathrm{G}})[\dot{x}_{\mathrm{G}}^2 + \dot{y}_{\mathrm{G}}^2 + \dot{z}_{\mathrm{G}}^2] \tag{13}$$

The internal mechanism swings slowly without a significant contribution to the system rotational kinetic energy and therefore the gyro-flywheel would be the main provider for the rotational energy in the pendulum mechanism which is given by:

$$T_{\mathrm{G}}^{\mathrm{r}} = \frac{1}{2}[(\omega_{\mathrm{Gx}})^2 I_{\mathrm{xxG}} + (\omega_{\mathrm{Gy}})^2 I_{\mathrm{yyG}} + (\omega_{\mathrm{Gz}})^2 I_{\mathrm{zzG}}] \tag{14}$$

where, ω_{Gx}, ω_{Gy} and, ω_{Gz} are the components of the gyro-flywheel angular speed (ω_G) with respect to the absolute coordinates. The potential energy of the gyro-flywheel and the pendulum mechanism is,

$$P_G = (m_P + m_G)(R\sin\beta - \iota\cos\theta\sin\beta)(g) \tag{15}$$

Finally the Lagrangian function of the system is

$$L = [T_w + (T_G^t + T_G^r)] - (P_w + P_G) \tag{16}$$

The dynamic equations for the entire system can be derived by substituting Equations (10-15) into Eq. (16). The general dynamic equation of the system is solved numerically using the Kutta-Merson integration. The solution is based on variable time step which automatically adjusts the time increment and monitor simulation errors of various types.
Because of the applied loadings, it may not be known if the robot wheel rolls without slipping or slides as it rolls. Such conditions are checked at each time increment during the robot simulation by investigating the dynamic balance between the resulted angular and linear inertia loads and the applied external torques and forces on the robot wheel using Newton's and Euler's Equations. The simulation detects collisions geometrically by finding the intersections between the bodies. When bodies collide, the simulation computes the forces and/or the impulses necessary to prevent interpenetration and applies these responses at the contact points. Based on the obtained values for these responses (forces and impulses) the program calculates the new accelerations and velocities of the bodies and continues the simulation process. The solution scheme is based on using appropriately small integration steps near collisions and employs an impulse momentum collision model with proper coefficient of restitution.

4. Controller Configuration

It is difficult to acquire a controller that ensures continuous trajectory tracking under stabilized condition for single wheel mobile robot under continuous exposal to an erratic real time inputs. The use of intelligent controller is generated by the random nature of system excitations which largely depends on unpredictable parameters such as friction, and other variable dynamic forces. A neural network can model the response of such system by means of a nonlinear regression in the discrete time domain. The result is a network, with adjustable weights, that might approximate the system dynamics. Though it is a problem since the knowledge is stored in an opaque fashion and the learning results in a large set of parameter values which almost impossible to be interpreted in words. Conversely using a fuzzy rule based controller that consists of readable if-then statements which is almost a natural language, cannot learn new rules alone. The neurofuzzy controller might be preferred over the others for such application since it combines the two and it has a learning architecture (Jang et al., 1997). To construct a neurofuzzy controller with ANFIS (Adaptive Neuro Fuzzy Inference System), we need a set of input-output data. In this work, two input signals are considered. The first input is the wheel orientation error (ε_β, OrientError) which is defined as the angle of deviation between the vertical line that passes through the ground contact point and the line that connects the wheel mass centre and wheel contact point. The second input is the deviation angle between the actual wheel path and the tangent to the

planned track (ε_α, DirectError). The output signals are the angular velocity of steering and balance motors as indicated in Figure 2. The gyro drive shaft is kept at constant angular velocity.
Control strategies under different design parameters that might be difficult to implement in a real experimental setup can be tested by using the dynamic simulation of ordinary Sugeno's Fuzzy controller. All problem components are integrated through visual basic as shown in Figures 3 and 5. Data set are collected for training and adapting the Neurofuzzy controller in the next stage. The cost effectiveness of such simulation is add to the important flexibility in exploring different dynamic parameters which might be difficult to introduce in actually built system.

4.1 Takagi-Sugeno model

The general Takagi-Sugeno rule structure is:
If g (e_1 is A_1, e_2 is A_2, . . . , e_k is A_k) then

$$y = f(e_1, e_2, \ldots, e_k) \tag{17}$$

Here f is the logical function which connects the sentences that form the implemented conditions, y is the output, and, f is a function of the inputs e_1, e_2, . . . , and e_k. The inputs in this work are the orientation and track errors, while the outputs are the angular velocity of steering motor and, balance motor.
The rules can be structured according to the importance of the actual parameters involved in the targeted application based on the simulated dynamic model. The Takagi and Sugeno's fuzzy model can be formulated as the following:

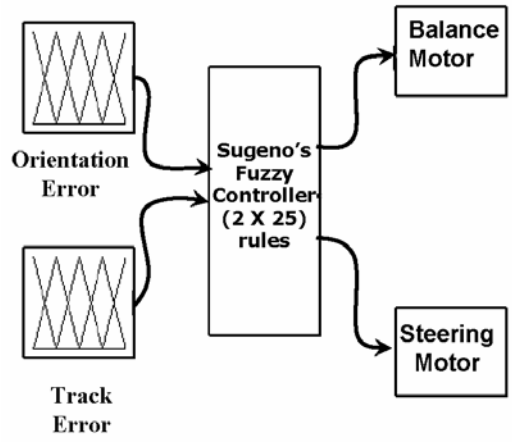

Figure 5. Sugeno's Controller layout

$$\begin{aligned} L^i: \ & \text{IF } e_1 \text{ is } A_1^i \text{ and } \ldots\ldots \text{and } e_k \text{ is } A_k^i \text{ THEN} \\ & y^i = f_i = a_0^i + a_1^i.e_1 + \ldots + a_k^i.e_k \end{aligned} \tag{18}$$

where, $L^i\,(i = 1,2,\ldots\ldots n)$ denotes the i-th rule, n is the number of fuzzy rules, y^i *or* f_i is the output from the i-th rule (implication), $a_{p\,(p = 0,1,\ldots,k)}^i$ are consequent parameters, e_1, e_2, . .

. , e_k are the input variables, and A_p^i are fuzzy sets whose membership functions are denoted by the same symbols as the fuzzy values. Given an inputs (e_1, e_2, . . . ,e_k) the final output of the fuzzy model is inferred by taking the weighted average of the f_i is:

$$y = \frac{\sum_{i=1}^{n} w_i f_i}{\sum_{i=1}^{n} w_i} \tag{19}$$

where $w_i \rangle 0$ and f_i is calculated for the input by consequent equation of the i-th rule, and the weight w_i implies the overall truth value of premise of the i-th rule for input calculated as

$$w_i = \prod_{p=1}^{k} A_p^i . e_p \tag{20}$$

4.2 The Neuro-fuzzy control algorithm

To facilitate the learning (or adaptation) of the Takagi-Sugeno fuzzy model, it is convenient to implement the fuzzy model into a framework of adaptive network that can compute gradient vectors systematically. The resultant network architecture called ANFIS (Adaptive Neuro-Fuzzy Inference System). ANFIS is described by a similar Takagi-Sugeno model with a single difference that in this case the inputs, e_1 (ε_β -OrientError) and, e_2 (ε_α - DirectError) are range values. The fuzzy set for ε_β being $\mathbf{A_1}$ = { NegLarg, NegSmall, Zero, PosSmall, PosLarg}, and fuzzy set for ε_α being $\mathbf{A_2}$ = { NegLarg, NegSmall, Zero, PosSmall, PosLarg}. Fig. 6 illustrate graphically the fuzzy reasoning mechanism to derive an output y from a given inputs ε_β and ε_α .

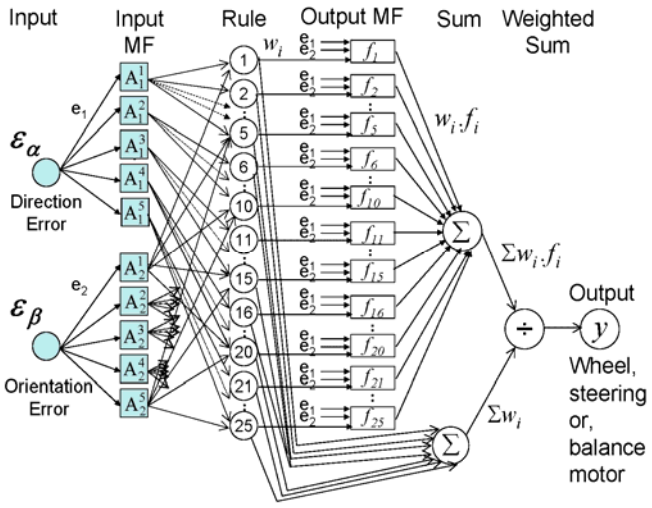

Figure 6. ANFIS architecture

ANFIS can have only one output y ; therefore three neurofuzzy controllers are implemented in order to obtain the required control command for the output motors. Output f_i is one of the motors angular speed for i-th rule where the size of the rule base is 25.
The dynamic simulation is conducted with several types and sizes of membership functions for the fuzzy sets $\mathbf{A_1}$ and, $\mathbf{A_2}$. Using triangular membership functions and a size of five for each of the two fuzzy sets were found the simplest and best suited for this case. The square elements in Fig. 6 represent the adaptive nodes depending on the parameter set of the adaptive network. The circles represent fixed nodes, which are independent of the parameter set. The first layer is composed of adaptive nodes representing the triangular membership functions (Jang et al., 1997) associated with each linguistic value. The second layer implements the fuzzy rules. Each node in this layer calculates the firing strength of a rule by means of multiplication between the membership degrees of the two inputs. The third layer consists of adaptive nodes which include the output membership.
The other two layers consist of fixed nodes that implement the weighted average procedure to obtain one of the motors output **y** as shown in Fig. 6. As the size of the rule base of the Sugeno fuzzy inference system (SFIS) is 25, we will have to identify 75 consequent parameters $\{ a_0^1, \ldots, a_0^{25}, a_1^1, \ldots, a_1^{25}, a_2^1, \ldots, a_2^{25} \}$ as indicated in Jang et al., (1997). This can be obtained from the neural network (NN) using training set $\{ \varepsilon_\beta, \varepsilon_\alpha, y \}$ which are collected from the dynamic simulation results by using the Sugeno fuzzy inference system. A back-propagation learning algorithm is used to identify these parameters in two steps. In the forward pass, the input membership functions are fixed and consequent parameters associated with the output are calculated by applying the least square estimation method. Using these parameters, the NN generates an estimate of the motor output. The difference between this estimate and the motor's value from the training set is then back-propagated in a second pass when the premise parameters associated with the input membership functions are calculated.

5. Simulation Results

In our simulation, we investigated the robot control tactics when passing a platform of three segments namely I, II, and, III as shown in Fig. 7. Segment-I in Fig. 7 (a) is used to investigate the robot capability in climbing an uphill ground or passing obstacle with adjustable tilt angle ψ both friction and restitution coefficients between the wheel and the uphill ground can be investigated. The uphill ground represented by the segment-I is kept with zero angular twist around the pathway centreline during results extractions. Segment-II represents the middle section of the platform with adjustable level relative to segment-I to investigate the jumping behaviour of the robot. Finally segment-III is the last section of the platform and twisted with an angle λ around the pathway centreline and used to examine manoeuvrability of the robot when it is confronted with sudden slop change of ground. Throughout our simulation the following physical, geometrical and mass parameters are used as given in Table 1

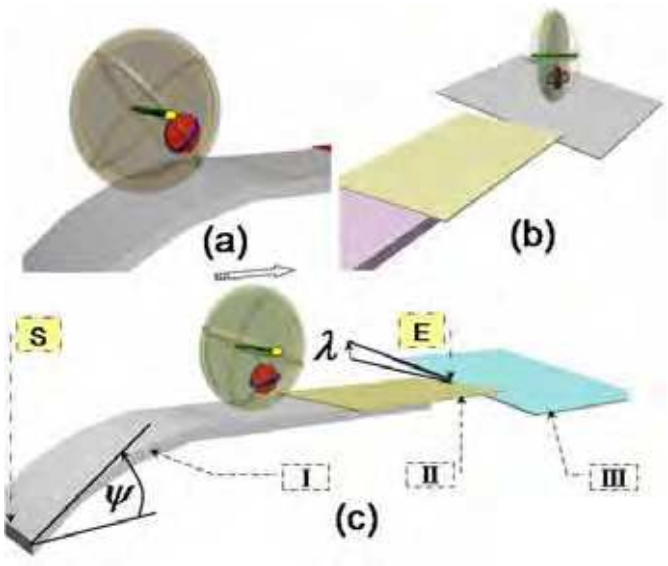

Figure 7. Simulation platform

Parameter	Designation	Value
The robot wheel mass	m	1.4 kg
The robot wheel radius	R	0.2 m
Gyro-wheel mass	m_G	5 kg
Gyro-wheel radius	r	0.06 m
Pendulum mechanism mass	m_P	2 kg
Pendulum length	ι	0.13 m
Friction coefficient-wet	μ_{k}	0.06-0.08
Friction coefficient-dry	μ_{d}	0.25-0.45
Coefficient of restitution	e	0.5-0.7

Table 2. Parameter values as shown in Fig. 4

Throughout the simulation our interest is concentrated on the application of ANFIS as adaptive control scheme and the results are compared to the Takagi-Sugeno fuzzy model. Our attempt is to establish a strategy to stand up a single wheel robot under large orient error angle ε_β. The trials failed either due to the high tilt rate requirement or the limited manoeuvring angle for the gyro.

Figs. 8 and 9 present the time variations in OrientError and DirectError angles for the single wheel robot under the Sugeno control.

The locations S and E are indicated in Fig. 7 on the simulation platform and the angles λ and ψ are 100^0 and 300^0 respectively.

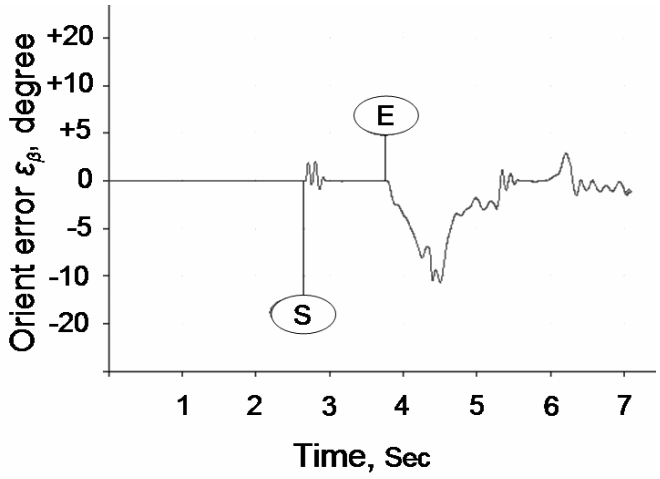

Figure 8 The time variation in orient error angle for λ =10^0 and ψ =30^0 under Sugeno control

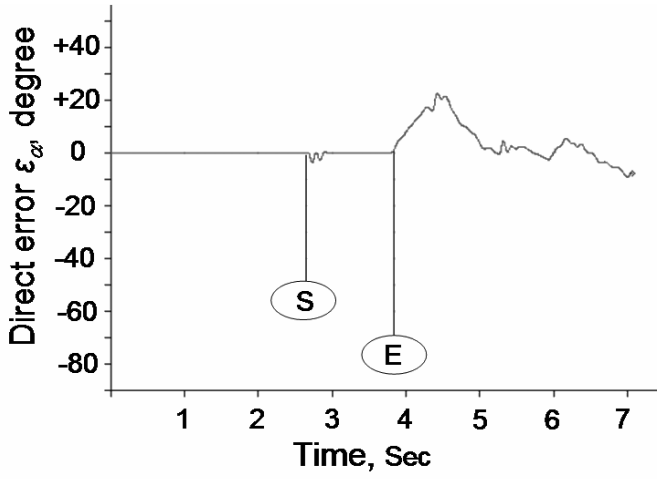

Figure 9 The time variation in direct error angle for λ =10^0 and ψ =30^0 under Sugeno control

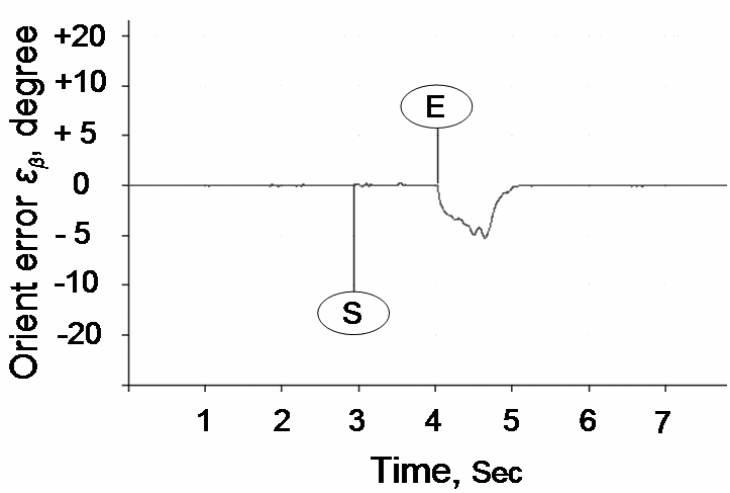

Figure 10 The time variation in orient error angle for λ =10^0 and ψ =30^0 under ANFIS control

Significant reductions for the variations of same angles under same simulation platform conditions are shown in Figs. 10 and 11 using the ANFIS control strategy.

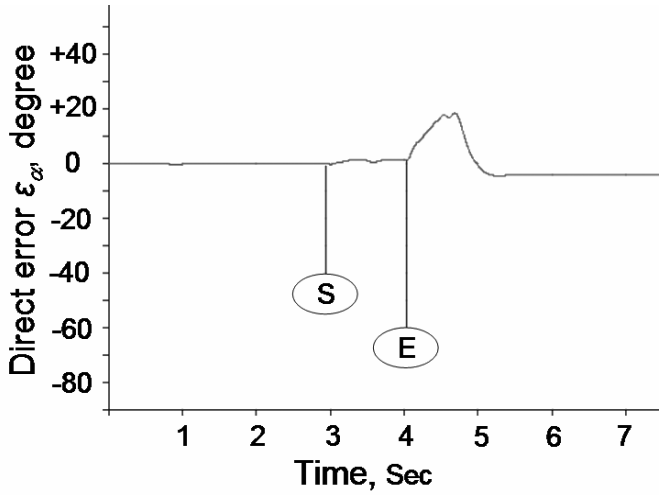

Figure 11 The time variation in direct error angle for λ =10^0 and ψ =30^0 under ANFIS control

By increasing the twist angle λ for segment-III to 30^0 the sugeno model couldn't keep the robot balance while the ANFIS controller proved a skilled performance in this aspect as indicated in Fig. 12.

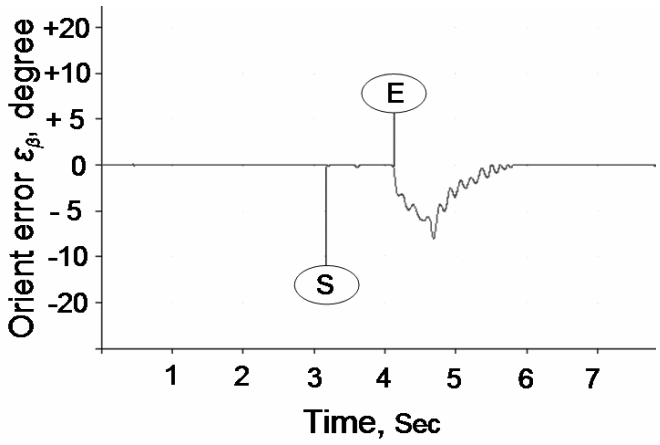

Figure 12 The time variation in orient error angle for λ =30^0 and ψ =30^0 under ANFIS control

6. Conclusions

The present work has proven the effectiveness of using the virtual prototyping and real time simulation in investigating the dynamic of a single wheel mobile robot under different manoeuvring tasks. Intelligent controller implementation has been shown to be effective in overcoming the difficulties raised from the unpredictable parameters such as friction, and other dynamic forces. The constructed neurofuzzy controller with ANFIS has indicated improvement over the Takagi-Sugeno fuzzy controller. The control tactics was tested with a robot passing a platform of three segments. The robot has shown capability in climbing an uphill ground or passing obstacle with different tilt angles where both friction and restitution coefficients between the wheel and the uphill ground can be implemented without any sophistications.

7. References

Autumn, K.; Sitti, M.; Liang, Y.A.; Peattie, A.M.; Hansen, W.R.; Sponberg, S.; Kenny, T.; Fearing, R.; Israelachvili, J.N. & Full, R.J. (2002), Evidence for van der Waals adhesion in gecko state, *Proceedings of the National Academy of Sciences,* Vol. 99, pp.12252-6.

Autumn, K.; Liang, Y.; Hsieh, T.; Zesch, W.; Chan, W.P.; Kenny, T.; Fearing, R. & Full, R.J. (2000), Adhesive force of a single Geckobot foot hair, *Nature*, Vol. 405, pp. 681-5.

Bloch, A.M. (2003), Nonholonomic Mechanics and Control, Springer.

Bretl, T.; Miller, T.; Rock, S. & Latombe, J.C. (2003), Climbing Robots in Natural Terrain, *7th Int. Symp. on Artificial Intelligence, Robotics and Automation in Space*, Nara, Japan.

Briones, L.; Bustamante, P. & Serna, M. (1994), ROBICEN: A wall-climbing pneumatic robot for inspection in nuclear power plants, *Robotics and Computer-Integrated Manufacturing,* vol. 11, pp. 287-292.

Cavin, R. D. (2001), Gyroscopically Stabilized and Controlled Single-Wheeled Autonomous Vehicle, *2000 Florida Conference on Recent Advances in Robotics (FCRAR 2000)*, May 10-11, FAMU/FSU, Tallahassee, Florida.

Ferreira, E.; Tsai, S.; Paredis, C.; & Brown, H. (2000), Control of the Gyrover: a single-wheel gyroscopically stabilized robot, *Advanced Robotics*, Vol. 14, No. 6, pp. 459 - 475.

Hirose, s. (1993), Biologically Inspired Robots: Snake-Like Locomotors and Manipulators, New York, NY, Oxford University Press.

Iagnemma, K. & Dubowsky, S. (2004), Traction Control of Wheeled Robotic Vehicles with Application to Planetary Rovers, *Intl Journal of Robotics Research*, Vol. 23, no. 10, pp. 1029-1040.

Jang, J.-S. R.; Sun, C.-T. & Mizutani, E. (1997), *Neuro-Fuzzy and Soft Computing*, Prentice Hall, ISBN 0-13-261066-3

Martynenko, Yu. G. & Formal'skii, A. M. (2005), A Control of the Longitudinal Motion of a Single-Wheel Robot on an Uneven Surface, *Journal of Computer and Systems Sciences International*, Vol. 44, No. 4, pp. 662-670

Nagakubo, A. & Hirose, S. (1994), Walking and running of the quadruped wall-climbing robot, *Proceedings of the IEEE International Conference on Robotics and Automation*, pp. 1005-1012.

Nandy, G. C. & Xu, Y. (1998), Dynamic model of a gyroscopic wheel, *Proc. IEEE Int. Conf. on Robotics and Automation*, pp. 2683-88, Leuven, Belgium.

Nukulwuthiopas, W.; Laowattana, D. & Maneewarn, T. (2002), Dynamic Modeling of a One-Wheel Robot By Using Kane's Method, *IEEE International Conference on Industrial Technology (IEEE ICIT '02)*, pp. 524-529, December 11-14, Bangkok, Thailand.

Pack, R.T.; Christopher, J.L. & Kawamura, K. (1997), A Rubbertuator-Based Structure-Climbing Inspection Robot, *Proceedings of the IEEE International Conference on Robotics and Automation*, pp. 1869-1874.

Rashid, M. K. & Khalil, Z. A. (2004), Configuration Design and Intelligent Stepping of a Spherical Motor in Robotic Joint, *Journal of Intelligent and Robotic Systems*, Volume 40, Issue 2, Pages 165 – 181..

Rashid, M. K. (2007), Simulation of Intelligent Single Wheel Mobile Robot, *International Journal of Advanced Robotic Systems*, ARS Publication, Vol. 4 No. 1 ISSN 1729-8806, pp.73-80.

Samuel, K. W. Au; Yangsheng, Xu & Wilson, W. K. Yu. (2001), Control of tilt-up motion of a single wheel robot via model-based and human-based controllers, *Mechatronics*, Vol. 11, pp. 451-473

Shah, G. & Sitti, M. (2004), Modeling and Design of Biomimetic Adhesives Inspired by Gecko Foot-Hairs, *Proc. of the IEEE Conf. on Robotics and Biomimetics*, Shenyang, China.

Shuliang, L.; Yanzheng, Z.; Xueshan, G.; Dianguo, X. & Yan, W. (2000), A wall-climbing robot with magnetic crawlers for sand-blasting, *Spray- Painting and Measurement High Technology Letters*, Vol. 10, 86-8.

Tokioka, S. & Sakai, S. (1988), Painting robot for wall surface, *Robot*, Vol. 65, 88-96.

Xu, Y.; Brown, H. B. &, Au, K. W. (1999), Dynamic Mobility with Single-Wheel Configuration, *The International Journal of Robotics Research*, Vol. 18, No. 7, pp. 728-738

Xu, Z. & Ma, P., (2002)A wall-climbing robot for labeling scale of oil tank's volume, *Robotica,* Vol. 20, 209-212.

Yangsheng Xu & Samuel, K. W. Ou (2004), Stabilization and path following of a single wheel robot, *IEEE/ASME Transactions on Mechatronics*, Vol. 9, No. 2, pp. 407-419.

Yanzeng, Z.; S. Hao, & Yan, W. (1999), Wall-climbing robot with negative pressure sucker used for cleaning work, *High Technology Letters,* Vol. 5, 85-88.

Bioinspiration and Robotics Walking and Climbing Robots

Edited by Maki K. Habib

ISBN 978-3-902613-15-8

Hard cover, 544 pages

Publisher I-Tech Education and Publishing

Published online 01, September, 2007

Published in print edition September, 2007

Nature has always been a source of inspiration and ideas for the robotics community. New solutions and technologies are required and hence this book is coming out to address and deal with the main challenges facing walking and climbing robots, and contributes with innovative solutions, designs, technologies and techniques. This book reports on the state of the art research and development findings and results. The content of the book has been structured into 5 technical research sections with total of 30 chapters written by well recognized researchers worldwide.

How to reference

In order to correctly reference this scholarly work, feel free to copy and paste the following:

Maki K. Rashid (2007). Armless Climbing and Walking in Robotics, Bioinspiration and Robotics Walking and Climbing Robots, Maki K. Habib (Ed.), ISBN: 978-3-902613-15-8, InTech, Available from: http://www.intechopen.com/books/bioinspiration_and_robotics_walking_and_climbing_robots/armless_climbing_and_walking_in_robotics

INTECH
open science | open minds

InTech Europe
University Campus STeP Ri
Slavka Krautzeka 83/A
51000 Rijeka, Croatia
Phone: +385 (51) 770 447
Fax: +385 (51) 686 166
www.intechopen.com

InTech China
Unit 405, Office Block, Hotel Equatorial Shanghai
No.65, Yan An Road (West), Shanghai, 200040, China
中国上海市延安西路65号上海国际贵都大饭店办公楼405单元
Phone: +86-21-62489820
Fax: +86-21-62489821